IL-33 receptor ST2 deficiency attenuates renal ischaemia–reperfusion injury in euglycaemic, but not streptozotocin-induced hyperglycaemic mice

M. Sehnine, M. Ferhat, S. Sena, J.M. Gombert, J.M. Goujon, A. Thierry, G. Touchard, T. Hauet, André Herbelin, Samy Hadjadj

Title: IL-33 receptor ST2 deficiency attenuates renal ischemia-reperfusion injury in euglycemic but not in streptozotocin-induced hyperglycemic mice

Running title: Alarmins, renal ischemia-reperfusion and hyperglycemia

M Sehnine [a,b,*], M Ferhat [a,b,*], S Sena [a,c], JM Gombert [a,b,c], JM Goujon [a,b,d], A Thierry [a,b,e], G Touchard [b,e] , T Hauet [a,b,c], A Herbelin [a,b,c,**], S Hadjadj [a,b,f,g**]

[*/**] both authors equally contributed to this manuscript

[a] INSERM U1082, Poitiers, France

[b] Université de Poitiers, UFR Médecine Pharmacie, Poitiers, France

[c] CHU Poitiers, Pôle BIOSPHARM, Poitiers, France

[d] CHU Poitiers, Department of Pathology, Poitiers, France

[e] CHU Poitiers, Department of Nephrology, Poitiers, France

[f] CHU Poitiers, Department of Endocrinology and Diabetology & CIC, Poitiers, France

[g] INSERM CIC 1402, Poitiers, France

Corresponding author:

Samy HADJADJ

CHU Poitiers, Department of Endocrinology and Diabetology, 2 Rue de la Milétrie, 86000 Poitiers, France

Phone: +33 5 49 44 21 82, Fax: +33 5 49 44 40 06

E-mail address: **samy.hadjadj@gmail.com**

Word count: 3127 ; Abstract: 249 words ; 2 Tables, 5 Figures,

Supplementary material: 1 table, 3 Figures

Key words: acute tubular necrosis, diabetic nephropathy, hyperglycemia, IL-33/ST2, inflammation, renal ischemia-reperfusion

Abbreviations : AKI, acute kidney injury; BMI, body mass index; BUN, blood urea nitrogen; GFR, glomerular filtration rate IRI, ischemia-reperfusion injury; HMBS, HydroxyMethylBilane Synthase; HPRT, hypoxanthine phosphoribosyl-transferase 1; PAS, periodic acid Schiff; RLP5, Ribosomal Protein L5; SD, standard deviation, STZ, streptozotocin; UAE, urinary albumin excretion; VEGF-A, vascular endothelial growth factor A; WT, wild-type

Abstract

Aim: Kidney hypoxia can predispose to the development of acute and chronic renal failure in diabetes. Ischemia-reperfusion injury (IRI) causes inflammation, and diabetes was found to exacerbate this inflammatory response in the kidney. The alarmin IL-33 could act as an innate immune mediator during kidney IRI. The aim of the present study was to examine the impact of genetic IL-33 receptor ST2 deficiency ($ST2^{-/-}$) on renal IRI in euglycemic and hyperglycemic mice.

Methods: Hyperglycemia was induced with streptozotocin (STZ) in adult male C57BL/6JRj wild-type (WT) mice and $ST2^{-/-}$ mice. Unilateral renal IRI was achieved after 3 months following STZ treatment, through left kidney nephrectomy (non-ischemic control kidney) and clamping of the right renal artery for 32 minutes of STZ- and Vehicle-treated animals. Twenty-four hours post-reperfusion, renal function and injury were determined by measurement of plasma creatinine, blood urea nitrogen (BUN) and histology scoring of tubules. In a complementary pilot study, soluble ST2 concentration was compared in diabetic and non-diabetic patients.

Results: Urinary albumin was significantly increased in STZ-induced hyperglycemic mice, regardless of genotypic background. Twenty-four hours post-ischemia, plasma creatinine, BUN and tubular injury were significantly reduced in $ST2^{-/-}$ mice compared to WT mice, in Vehicle-treated animals but this protective effect was lost in STZ-induced hyperglycemic $ST2^{-/-}$ animals. Plasma concentration of soluble ST2 were significantly in type 2 diabetic vs non-diabetic patients.

Conclusion: Our data suggest that the IL-33/ST2 pathway exerts differential effects depending on glucose environment, opening new avenues for further research on alarmins and diabetes in ischemia-related diseases.

Introduction

Diabetes mellitus is a chronic condition whose incidence and prevalence are rapidly increasing globally [1] with chronic renal complications associated in approximately one third of affected patients [2]. In addition to its impact on long-term complications, diabetes is a risk factor for acute kidney injury (AKI) [3]. Recently, diabetes emerged as a risk factor for renal hypoxia, probably linking acute kidney injury and diabetes [4]. Renal ischemia-perfusion injury (IRI) is an important condition, which can act in conjunction with hyperglycemia to favor the development of diabetic nephropathy [5]. The link between IRI and diabetes is supported by animal models in which acute transient hyperglycemia increases renal IRI [6, 7]. The relationship between IRI and chronic kidney disease in diabetes is not fully understood but might involve pro inflammatory pathways, as supported by data in obese diabetic rats [8].

The cytokine/alarmin Interleukin 33 (IL-33), a member of the IL-1 cytokine family, is released by endothelial and epithelial cells under stress and necrosis and recognized by the immune system as an endogenous danger signal [8-10]. The recent demonstration that IL-33 contributes to cisplatin-induced acute kidney injury [11] leads to hypothesize that IL-33 acts as an innate immune mediator during kidney IRI. Indeed, IL-33 targets iNKT cells, NK cells, polynuclear neutrophils and monocytes/macrophages [8, 9] that are involved in the development of kidney IRI [12]. IL-33 binds to both isoforms of the ST2 receptor, the transmembrane isoform (ST2 or ST2L) and the soluble isoform (sST2). ST2 heterodimerizes with IL-1 receptor accessory protein (IL-1RAcP) to transduce IL-33 signals [9].

The role of the IL-33/ST2 pathway was shown to be important in cisplatin-induced AKI [11] while a deleterious impact of diabetes was previously established in renal IRI [6, 7]. However, the relationship between alarmins and diabetes is largely unknown. Thus, the aim of our study was to evaluate the impact of renal IRI in IL-33 receptor ST2-deficient mice ($ST2^{-/-}$), in the context of streptozotocin (STZ)-induced diabetes. We also determined the

plasma concentration of sST2 in diabetic and control subjects, in a complementary pilot study.

Material and Methods

Study animals and surgical procedures

Eight to twelve-week-old male wild-type (WT) C57BL/6JRj and mutant ($ST2^{-/-}$) mice were used and bred in our animal facility (UFR Medicine, Poitiers) under specific pathogen-free conditions. $ST2^{-/-}$ mice were generated as previously described [13] and backcrossed onto the C57BL/6JRj background for 12 generations.

Hyperglycemia was induced by intraperitoneal injections of STZ (50 mg/kg/day for 5 consecutive days) or vehicle (sodium citrate buffer) as previously described by the AMDCC consortium (http://www.diacomp.org/shared/document.aspx?id=19&docType=Protocol). Animals were screened for blood glucose, sampled from the caudal vein, using a Bayer glucometer to ensure chronic hyperglycemia, after a 4-hour fast.

IRI experiments were performed at 5 months of age. Animals were anaesthetized with isoflurane. Temperature control was set at 37°C. A flank incision was performed and a left unilateral nephrectomy was performed, allowing access to renal tissue at baseline (D0). IRI was performed on the right kidney by 32 minutes clamping of the renal pedicle followed by 24 hours reperfusion (D1). Blood and renal tissue were then collected. All procedures were performed in accordance with the recommendations of the European Accreditation of Laboratory Animal Care and French institutional committee (CEEA-122: 2012-06).

Renal function tests

Mice were kept in an individual metabolic cage for 24-hour urine collection, 2 days before surgical procedure. Urinary albumin excretion (UAE) on 24-hour urine collection was determined with an immunoturbidimetric method. Urinary and blood glucose were determined using a glucose oxidase method. Blood samples were collected from retroocular vein plexus. Creatinine and blood urea nitrogen were determined using a modified Jaffe's method and a colorimetric method, respectively on a Modular System P (Roche Diagnostics GmbH, Mannheim, Germany).

Histological preparation

One half of the kidney was fixed in 4% paraformaldehyde. Paraffin-embedded tissues were stained with periodic acid Schiff (PAS) and examined using an Olympus BX51 microscope. A renal pathologist, blinded to experimental conditions, evaluated the presence of acute tubular necrosis in tubular proximal cell, according to three different criteria: tubular dilatation, cell detachment and loss of brush border, using a semi quantitative scoring, in a 5-scale numerical score as follows: 0: no lesion; 1: lesions affecting less than 25% of kidneys samples; 2: lesions affecting 25-50% of kidney samples; 3: lesions affecting 50-75% of kidney samples; 4: lesions affecting more than 75% of kidney samples [14]. Detection of immune cell infiltrates was carried on PAS-stained tissues.

RNA extraction and Real-Time Quantitative Reverse Transcription PCR (qRT-PCR)

Total RNA was extracted from mouse kidney tissue using the Nucleospin RNA Extraction kit, according to the manufacturer's instructions (Macherey-Nagel). One microgram of RNA was then retro-transcribed using the qScript cDNA Supermix (Quanta Biosciences). Quantitative real-time PCR were performed with the 2X Perfecta SYBR Green Mix (Quanta Biosciences), using the Rotor-Gene Q Lightcycler (Qiagen). For each primer pair used, PCR efficiency was

determined and integrated to calculate relative mRNA quantity against a standard curve. We evaluated six housekeeping genes (β-actin, hypoxanthine phosphoribosyl-transferase 1 (HPRT), Ribosomal Protein L5 (RLP5), non-POU-domain-containing, octamer binding protein (Nono), HydroxyMethylBilane Synthase (HMBS) and vascular endothelial growth factor A (VEGF-A) to determine the reference gene most suitable to normalize the Cp value of IL-33 and MCP-1 genes with the same set of kidney samples from euglycemic and hyperglycemic WT mice. Results were then normalized against VEGF-A as a loading control (identified as the most stably expressed gene according to the averaged expression stability values). See Supplemental Table for primer sequences and accession numbers.

Patients and plasma sST2 quantification

Plasma sST2 concentrations were compared in patients with diabetes *vs* non-diabetic patients. Blood samples were collected in a fasted state and stored at -80°C, until used at the Poitiers CRB 0033-00068. All patients gave written informed consent and the biobanking project (Biobanque Maladies Métaboliques) was approved by the local ethics committee (CPP Ouest 3). The type of diabetes was determined according to clinical factors (age at diagnosis below 40 years in type 1, above in type 2 diabetes), the time for definitive insulin requirement (lower than 1 year in type 1, higher than 2 years in type 2).

Diabetic nephropathy was classified according to urinary albumin concentration as absent (normoalbuminuria), incipiens (microalbuminuria) and established (proteinuria).

Non-diabetic controls were matched with T2DM patients on age (+/- 5 years) and sex. They originated either from a study of healthy volunteers or from patients from the Poitiers Biobank, hospitalized for non-malignant adrenal incidentaloma or pituitary disease, without conditions such as infection, inflammatory disease or cancer.

Plasma sST2 levels were measured using the Quantikine Human ST2/IL33 R Immunoassay (R&D Systems), according to the manufacturer's instructions.

Statistical analysis

Data are given as means ± SD (SEM in figures) or median (minimum-maximum) if not normally distributed. Comparison between animal groups was performed using an ANOVA or Kruskal-Wallis test, if data were skewed. qRT-PCR data were compared using a 1-Way ANOVA test followed by a Tukey's multiple comparison analysis. Patients with and without diabetes were compared using unpaired student t-test and chi-2 tests for categorical variables. Animal and human analyses were performed using GraphPad Prism version 5.01 software (San Diego California USA) and Statview 5 software (SAS Institute, Cary, NC, USA), respectively. P value at 0.05 was considered as statistically significant.

Results

1- Baseline characteristics

Baseline clinical and biological characteristics of WT and ST2$^{-/-}$ mice are presented in Table 1. As expected, blood glucose concentration was higher in STZ-treated mice. Hyperglycemic animals had a significantly decreased body weight and significantly higher kidney weight and kidney weight/body weight ratio compared with euglycemic animals. Of note, ST2$^{-/-}$ mice were leaner than WT mice even though STZ-treated ST2$^{-/-}$ and WT mice were not significantly different regarding renal parameters.

Urinary albumin excretion rates are presented in Figure 1. As expected, UAE was higher in hyperglycemic mice. Interestingly, in mice with hyperglycemia, urinary albumin was higher in ST2$^{-/-}$ than in WT mice. However, glomerular histology showed no mesangial expansion in hyperglycemic animals regardless of WT and ST2$^{-/-}$ genotype (Supplementary Figure 1).

Using qRT-PCR, we found an increased renal gene expression of IL-33 (IL-33/VEGF-A mRNA ratio; relative values) in kidneys from hyperglycemic *vs* euglycemic WT mice (1.00 ± 0.19 vs 1.49 ± 0.47, respectively; P = 0.023).

2- Effect of renal IRI

Renal function was analyzed 24 hours after renal IR procedure. Of note, none of the mice died before IR sequence and no mortality was found before 24 hours. As expected, plasma creatinine (Figure 2) and BUN (Figure 3) levels were significantly higher post-IR compared to baseline in both STZ-treated and euglycemic WT mice. In contrast to WT mice for which no difference in serum creatinine and BUN levels was found between euglycemic and hyperglycemic phenotypes, their counterpart levels in ST2$^{-/-}$ mice were lower in euglycemic compared to hyperglycemic mice (Figure 2 and Figure 3). When comparing control euglycemic ST2$^{-/-}$ and WT animals, both serum creatinine and BUN levels post-IR were

significantly lower in $ST2^{-/-}$ mice compared to their WT counterparts. This protective effect was not maintained in hyperglycemic animals, in which serum creatinine (Figure 2) and BUN levels (Figure 3) post-IR did not differ between $ST2^{-/-}$ and WT mice.

A similar conclusion was obtained when considering histological features of acute tubular injury (Figure 4 and Supplementary Figure 2) showing a statistically significant protective effect provided by the lack of ST2 in euglycemic control animals but not in hyperglycemic animals.

As shown in Figure 5, mRNA levels of the MCP-1/CCL2 chemokine, responsible for monocyte/macrophage and neutrophil recruitment to inflammatory sites, were significantly higher post-IR compared to baseline in both STZ-treated and euglycemic WT mice. In contrast to WT mice, for which no difference in MCP-1 mRNA levels was found between euglycemic and hyperglycemic phenotypes, their counterpart levels in $ST2^{-/-}$ mice were lower in euglycemic compared to hyperglycemic mice.

In euglycemic WT mice, IR was accompanied by moderate but significant polynuclear cell infiltrates, a phenomenon which was lost in their $ST2^{-/-}$ counterparts (Supplementary Figure 3). Immune cell recruitment was found attenuated in post-IRI kidneys of hyperglycemic WT mice, while it remained low in hyperglycemic post-IRI kidneys of $ST2^{-/-}$ mice, showing no clear difference with their euglycemic counterparts.

3- Pilot study: sST2 in diabetic and non-diabetic patients

The comparison between diabetic and non-diabetic patients is presented in Table 2. Briefly type 1 diabetes patients were leaner than patients with type 2 diabetes. We found a modest significant difference in sST2 concentrations between male and female participants: 15.01 ng/ml (5.79-30.03) and 13.08 (5.99-72.89); P=0.0363, respectively.

We found that the plasma concentration of sST2 was different in diabetes patients compared with matched controls with borderline signification: 14.73 ng/ml (5.79-72.89) and 13.07 (5.99-43.20); P=0.0606, respectively, while the difference was significant when comparing non-diabetes controls and patients with type 2 diabetes (P=0.0258) (see Table 2). In addition, no significant difference was evidenced regarding sST2 concentration between those patients with or without diabetic nephropathy: 14.27 (5.79-72.89), 17.27 (9.18-25.84) and 17.73 (10.02-30.03) ng/ml; P=0.199, in patients without nephropathy (n=67, with 33 in type 2 diabetes patients), with incipient nephropathy (n=10, all in type 2 diabetes patients) and in established nephropathy (n=11, all in type 2 diabetes patients), respectively, although a weak correlation was found with urinary albumin concentration (Rho: 0.225; P=0.03).

We found no significant correlation between sST2 concentration and BMI (Rho: -0.076; P=0.361), age (Rho: 0.013; P=0.876) or CKD-EPI estimated GFR (Rho: -0.021; P=0.795).

Discussion

Our data showed that the defect of ST2, which is expected to lead to a lack of transmission of alarmin signals mediated by IL-33 was associated with a reduced kidney injury profile after a renal IR sequence, as attested by decreased levels of serum creatinine, BUN, attenuated polynuclear cell infiltration, and lesser histology scores of tubular injury. However, this protective effect was not maintained in hyperglycemic animals.

The finding that the lack of ST2 was associated with a reduced renal injury 24-hours after renal ischemia suggests that the deletion of the signalization of the IL-33 alarmin reduces acute renal injury. This is in line with the known effects of IL-33, which is released in response to cell stress, and whose function is to indicate to target cells of an injury requiring either reparation or apoptosis [9]. This is consistent with data generated in another model of AKI (cisplatin-induced) where administration of IL-33 was associated with more severe renal injury [11].

Although reported for the first time, to our knowledge, our results of a protective effect according by genetic deletion of ST2 in renal IRI are suitable with the commonly described role of alarmins. However, the finding of a loss of this protective effect in hyperglycemic animals was unexpected, leading us to speculate that IL-33 exerts differential effects depending on glucose environment [9].

In addition to the difference in ischemic acute kidney injury, the findings that baseline urinary albumin excretion was increased in long-term chronic hyperglycemic $ST2^{-/-}$ compared to WT was unexpected and can be a possible marker of chronic kidney disease, even though we could not evidence any difference in glomerular structure (see Supplementary Figure 1). This suggests a differential involvement of ST2 in acute and chronic situations, requiring further investigations.

We found that glycosuria was greater in $ST2^{-/-}$ animals than in the WT counterparts, while this phenotype was totally unexpected. It proved to be true in diabetic setting; a similar trend was found in non-diabetic animals, though non-significant. As blood glucose was not different in $ST2^{-/-}$ and WT mice, we can speculate that ST2 could interfere with tubular glucose reabsorption, and possibly with SGLT pathways. However, this is completely beyond the scope of the paper and might deserve further attention in the future.

We speculate that the IL-33/ST2 pathway could already be up-regulated in hyperglycemic mice, as supported by our data showing an increased local gene expression of IL-33 in kidney of hyperglycemic *vs* euglycemic WT mice, in accordance with a recent finding [15]. On the other hand, since hyperglycemia was previously shown to be associated with low-grade inflammation [16], we cannot exclude adaptive mechanisms leading to differential IL-33 signaling. These two non-exclusive hypotheses could explain why when hyperglycemia is induced, an increase in urinary albumin and a higher susceptibility to IRI were selectively found in $ST2^{-/-}$ animals.

The molecular effectors responsible for this differential effect of the IL-33/ST2 pathway were searched. We focused our analyses on transcripts involved in the inflammation pathway, such as MCP-1, ICAM-1 and VCAM-1. We were able to evidence renal *MCP-1* gene expression, paralleling biological and histological findings, with a significant increase during IR in WT animals and in $ST2^{-/-}$ hyperglycemic mice (Figure 5). As MCP-1 is known to drive myeloid cell recruitment, we expected an immune cell infiltration paralleling renal acute tubular necrosis. However, we found a dissociation between MCP-1 mRNA and immune cell infiltration, with no infiltration particularly in WT-hyperglycemic mice. Of note, in WT-VEH mice, IR was accompanied by a moderate immune cell infiltration, far from a severe inflammatory condition.

The differential protective effect on renal IRI between WT and $ST2^{-/-}$ STZ-treated mice could depend on hyperglycemia or on renal injury or both. We acknowledge that there is a statistically significant difference in urinary albumin between euglycemic and hyperglycemic mice. However, this difference was not associated with any glomerular lesion in favor of an early diabetic nephropathy stage.

From our data in mice, it is tempting to speculate that the IL-33/ST2 pathway is deregulated in diabetic patients. The possible direct impact of STZ on IL33/ST2 pathway is impossible to distinguish in our model from the impact of long-term hyperglycemia. The reproduction of our findings in a non-toxic model of hyperglycemia such as genetically selected mice (ob/ob or Akita mice) might help to clarify this point. Regarding our observational pilot study, the concentrations of circulating sST2, commonly considered a functional signature of IL-33 signaling *in vivo*, did not strongly differ according to diabetes and nephropathy status. To our knowledge, the relationship between high glucose and the alarmin system was not searched in details in experimental setting, and only few studies were reported, showing a significant effect of diabetes and gender on sST2 serum concentration rather consistent with our findings [17, 18] [19]. Although diabetes-related inflammation is a likely pathway linking chronic hyperglycemia to endothelial and epithelial damage [20, 21], ultimately leading to a vicious circle of more inflammation-driven damage [20], here we could not find a relevant metabolic pathway linking glucose and alarmins, leaving this question open.

A remaining question is whether the IL-33/ST2 pathway has an impact not only in the early post-reperfusion phase of renal IRI, as demonstrated here 24 hours post-IRI, but also in the subsequent phase of tissue repair/remodeling. Indeed, IL-33 is involved in the development of fibrous tissue, as reported during chronic inflammation in lung [22]. On the other hand, by its

capacity to induce angiogenesis [23], IL-33 might act as a repair factor much later than the IR phase.

The consequences of our findings in clinical setting must be examined. The inhibition of alarmins could be a good strategy to prevent IRI and thus represent a possible therapeutic avenue, in AKI, particularly in non-diabetic persons. This point will be examined with future developments of some drugs targeting this pathway. However, a second consequence of our findings is that they give some impetus to search for the relationship between glucose and alarmins, as this aspect might be involved in the relationship between AKI and diabetes, considering the deleterious impact of AKI in diabetes patients [24].

Disclosure of interest

No potential conflict of interest relevant to this article was reported.

Acknowledgments

We thank Jeffrey Arsham for editing the English of our manuscript. We thank Aurélie Robin, Sébastien Giraud and the staff of U1082 for their kind technical support, Michèle Grosdenier and Sonia Brishoual (CRB 0033-00068) for their help with human samples. This study was supported by INSERM, CHU de Poitiers, Université de Poitiers, Association pour la Recherche en Immunologie-Poitou-Charentes (ARIM-PC, France), Groupement pour l'Etude des Maladies Métaboliques et Systémiques (GEMMS, Poitiers, France) and Ministère de la Recherche. $ST2^{-/-}$ mice are a kind gift of A. McKenzie (Laboratory of Molecular Biology, Cambridge, UK).

References

[1] Collaboration NCDRF. Worldwide trends in diabetes since 1980: a pooled analysis of 751 population-based studies with 4.4 million participants. Lancet 2016;387(10027):1513-30.

[2] Rossing P. Prediction, progression and prevention of diabetic nephropathy. The Minkowski Lecture 2005. Diabetologia 2006;49(1):11-9.

[3] Hertzberg D, Sartipy U, Holzmann MJ. Type 1 and type 2 diabetes mellitus and risk of acute kidney injury after coronary artery bypass grafting. Am Heart J 2015;170(5):895-902.

[4] Takiyama Y, Haneda M. Hypoxia in diabetic kidneys. Biomed Res Int 2014;2014:837421.

[5] Chawla LS, Kimmel PL. Acute kidney injury and chronic kidney disease: an integrated clinical syndrome. Kidney Int 2012;82(5):516-24.

[6] Goor Y, Peer G, Iaina A, Blum M, Wollman Y, Chernihovsky T, et al. Nitric oxide in ischaemic acute renal failure of streptozotocin diabetic rats. Diabetologia 1996;39(9):1036-40.

[7] Podrazik RM, Natale JE, Zelenock GB, D'Alecy LG. Hyperglycemia exacerbates and insulin fails to protect in acute renal ischemia in the rat. J Surg Res 1989;46(6):572-8.

[8] Kelly KJ, Burford JL, Dominguez JH. Postischemic inflammatory syndrome: a critical mechanism of progression in diabetic nephropathy. Am J Physiol Renal Physiol 2009;297(4):F923-31.

[9] Molofsky AB, Savage AK, Locksley RM. Interleukin-33 in Tissue Homeostasis, Injury, and Inflammation. Immunity 2015;42(6):1005-19.

[10] Liew FY, Girard JP, Turnquist HR. Interleukin-33 in health and disease. Nat Rev Immunol 2016;16(11):676-89.

[11] Akcay A, Nguyen Q, He Z, Turkmen K, Won Lee D, Hernando AA, et al. IL-33 exacerbates acute kidney injury. J Am Soc Nephrol 2011;22(11):2057-67.

[12] Jang HR, Rabb H. Immune cells in experimental acute kidney injury. Nat Rev Nephrol 2015;11(2):88-101.

[13] Townsend MJ, Fallon PG, Matthews DJ, Jolin HE, McKenzie AN. T1/ST2-deficient mice demonstrate the importance of T1/ST2 in developing primary T helper cell type 2 responses. J Exp Med 2000;191(6):1069-76.

[14] Goujon JM, Hauet T, Menet E, Levillain P, Babin P, Carretier M. Histological evaluation of proximal tubule cell injury in isolated perfused pig kidneys exposed to cold ischemia. J Surg Res 1999;82(2):228-33.

[15] Onk D, Onk OA, Turkmen K, Erol HS, Ayazoglu TA, Keles ON, et al. Melatonin Attenuates Contrast-Induced Nephropathy in Diabetic Rats: The Role of Interleukin-33 and Oxidative Stress. Mediators Inflamm 2016;2016:9050828.

[16] Stehouwer CD, Gall MA, Twisk JW, Knudsen E, Emeis JJ, Parving HH. Increased urinary albumin excretion, endothelial dysfunction, and chronic low-grade inflammation in type 2 diabetes: progressive, interrelated, and independently associated with risk of death. Diabetes 2002;51(4):1157-65.

[17] Caporali A, Meloni M, Miller AM, Vierlinger K, Cardinali A, Spinetti G, et al. Soluble ST2 is regulated by p75 neurotrophin receptor and predicts mortality in diabetic patients with critical limb ischemia. Arterioscler Thromb Vasc Biol 2012;32(12):e149-60.

[18] Miller AM, Purves D, McConnachie A, Asquith DL, Batty GD, Burns H, et al. Soluble ST2 associates with diabetes but not established cardiovascular risk factors: a new inflammatory pathway of relevance to diabetes? PLoS One 2012;7(10):e47830.

[19] Coglianese EE, Larson MG, Vasan RS, Ho JE, Ghorbani A, McCabe EL, et al. Distribution and clinical correlates of the interleukin receptor family member soluble ST2 in the Framingham Heart Study. Clin Chem 2012;58(12):1673-81.

[20] Lopes-Virella MF, Carter RE, Gilbert GE, Klein RL, Jaffa M, Jenkins AJ, et al. Risk factors related to inflammation and endothelial dysfunction in the DCCT/EDIC cohort and their relationship with nephropathy and macrovascular complications. Diabetes care 2008;31(10):2006-12.

[21] Nguyen DV, Shaw LC, Grant MB. Inflammation in the pathogenesis of microvascular complications in diabetes. Front Endocrinol (Lausanne) 2012;3:170.

[22] Li D, Guabiraba R, Besnard AG, Komai-Koma M, Jabir MS, Zhang L, et al. IL-33 promotes ST2-dependent lung fibrosis by the induction of alternatively activated macrophages and innate lymphoid cells in mice. J Allergy Clin Immunol 2014;134(6):1422-32 e11.

[23] Choi YS, Choi HJ, Min JK, Pyun BJ, Maeng YS, Park H, et al. Interleukin-33 induces angiogenesis and vascular permeability through ST2/TRAF6-mediated endothelial nitric oxide production. Blood 2009;114(14):3117-26.

[24] Monseu M, Gand E, Saulnier PJ, Ragot S, Piguel X, Zaoui P, et al. Acute Kidney Injury Predicts Major Adverse Outcomes in Diabetes: Synergic Impact With Low Glomerular Filtration Rate and Albuminuria. Diabetes care 2015;38(12):2333-40.

Table 1: Baseline characteristics of WT and ST2$^{-/-}$ mice with and without STZ-induced hyperglycemia

	WT		**ST2 - /-**		***P value***			
	Vehicle (**n=8**)	STZ (**n=8**)	Vehicle (**n=8**)	STZ (**n=8**)	a *vs* b	c *vs* d	a *vs* c	b *vs* d
	a	b	c	d				
Body weight (g)	33.76 ± 0.99	24.89 ± 0.82	30.23 ± 0.43	25.70 ± 0.83	P<0.0001	P= 0.0019	P= 0.0117	P= 0.6058
Left kidney weight (mg)	195 ± 7	209 ± 6	168 ± 3	180 ± 5	P= 0.1031	P= 0.0291	P= 0.007	P= 0.0093
Left kidney weight /body weight Ratio (mg/g)	5.78 ± 0.09	8.45 ± 0.36	5.57 ± 0.10	7.06 ± 0.29	P<0.0001	P= 0.0011	P= 0.1949	P= 0.0206
Blood glucose (mg/dL)	226 ± 14	567 ± 19	191 ± 16	574 ± 25	P<0.0001	P= 0.0002	P=0.1304	P= 0.7653
Urinary glucose (mg/dL)	284 ± 94	6461 ± 381	443 ± 130	9733 ± 574	P<0.0001	P<0.0001	P= 0.2786	P= 0.0002
Urinary glucose output (mg/24 hrs)	3.5 ± 1.5	169 ± 36	6.4 ± 1.6	828 ± 95	P<0.0001	P<0.0002	P= 0.1949	P= 0.0001

Table 2: Clinical and biological characteristics in controls and patients with diabetes

	T1	T2	Controls	P value			
	N=37	N=60	N=60	all 3 groups	T1 vs T2	T1 vs Controls	T2 vs Controls
Age (yrs)	61.5 +/- 8.7	66.3 +/- 9.4	65.4 +/- 9.7	0.508	**<0.0001**	0.0536	0.599
Sex (M//F)	18//19	30//30	30//30	0.832	0.897	0.897	-
Body mass index (Kg/m^2)	25.3 +/- 3.7	33.4 +/- 5.1	25.8 +/- 5.2	**<0.0001**	**0.0014**	0.625	**<0.0001**
Serum sST2 (ng/ml)	14.43 (5.79-27.91)	15.19 (6.05-72.89)	13.07 (5.99-43.20)	**0.0497**	0.116	0.558	**0.0258**
SBP (mm Hg)	123 +/- 25	126 +/- 15	124 +/- 16	0.730	0.645	0.702	0.624
DBP (mm Hg)	68 +/- 16	70 +/- 11	74 +/- 9	0.0546	0.484	0.0291	**0.045**
HbA1c (%)	7.9 +/- 1.4	7.5 +/- 1.2	-	-	0.139	-	**0.0018**
Serum creatinine (umol/l)	75 +/- 13	105 +/- 62	73+/- 16	**0.0013**	**0.0025**	0.495	0.877
eGFR (ml/min/1.73m^2)	86 +/- 14	68 +/- 27	73 +/- 15	**0.0004**	**<0.0001**	**<0.0001**	0.274

T1, is for patients living with type 1 diabetes (T1DM)
T2, is for patients living with type 2 diabetes (T2DM)
Data are means +/ SD or medians (min-max) if not normally distributed
sST2, soluble ST2; SBP/DBP, systolic/diastolic blood pressure

Figure legends

Figure 1: Urinary albumin excretion in WT and ST2$^{-/-}$ mice with euglycemia or STZ-induced hyperglycemia. Data are means and error bars are SEM (n=8 mice per group). ns, non-significant; * $P < 0.05$, *** $P < 0.0001$ (Mann-Whitney test for between group comparison).

Figure 2: Serum creatinine in WT and ST2$^{-/-}$ mice with euglycemia or STZ-induced hyperglycemia. D0 data correspond to baseline data. D1 data correspond to data 24 hours after reperfusion following 32 minutes warm-ischemia. Data are means and error bars are SEM (n=8 mice per group). ns, non-significant; * $P < 0.05$, ** $P < 0.001$, *** $P < 0.0001$ (Mann-Whitney test for between group comparison).

Figure 3: Blood urea nitrogen in WT and ST2$^{-/-}$ mice with euglycemia or STZ-induced hyperglycemia. D0 data correspond to baseline data. D1 data correspond to data 24 hours after reperfusion following 32 minutes warm-ischemia. Data are means and error bars are SEM (n=8 mice per group). ns, non-significant; * $P < 0.05$, ** $P < 0.001$, *** $P < 0.0001$ (Mann-Whitney test for between group comparison)

Figure 4: Acute tubular necrosis staging in WT and ST2$^{-/-}$ mice with euglycemia or STZ-induced hyperglycemia. D0 data correspond to baseline (control kidney obtained by left nephrectomy). D1 data correspond to data 24 hours after reperfusion, following 32 minutes warm-ischemia. Data are means and error bars are SEM (n=8 mice per group). ns, non-significant; * $P < 0.05$, ** $P < 0.001$, *** $P < 0.0001$ (Mann-Whitney test for between group comparison).

Figure 5: MCP-1 mRNA expression levels in wild-type and ST2$^{-/-}$ mice kidneys following IR injury. RTqPCR data of MCP1 mRNA expression normalized to VEGFA mRNA are presented. Statistical analysis was carried using 1-Way ANOVA test, followed by a Tukey's multiple comparison test. n=6-9 mice per group; *** $P < 0.001$, ns: non-significant.

Supplementary Figure 1

A: Representative glomerular involvement at baseline. Illustrative light microscopy on PAS stained kidney cortex of WT and ST2$^{-/-}$ mice with or without STZ-induced hyperglycemia at baseline.

B: Glomerular diameter at baseline (3 months post-treatment with vehicle and STZ) The average diameter of the glomeruli was assessed by quantification of 10 glomeruli per mouse using the same magnification. Data are means and error bars are SEM (n=8 mice per group)

Supplementary Figure 2: Representative histological findings at baseline and at D1 (24 hours after reperfusion, following 32 minutes warm-ischemia). Light microscopy on PAS stained kidney samples. Arrows represent typical acute tubular necrosis with extensive tubular dilation.

Supplementary Figure 3: Representative histopathological examination of kidneys from wild-type (WT) and ST2$^{-/-}$ mice, at baseline (D0) and 24 hr post ischemia/reperfusion challenge (D1). Light microscopy on Periodic Acid-Schiff (PAS) stained kidney samples is shown. Arrows point polynuclear cells recruited at the site of severe tubular necrosis. Asterisk indicate acute tubular necrosis with extensive tubular dilation.

Figure 1:

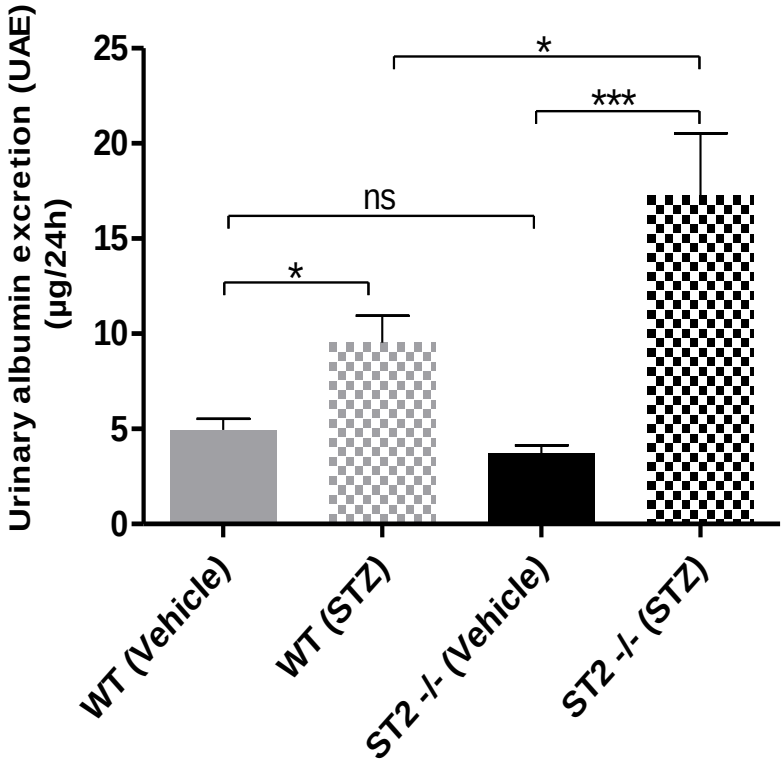
Urinary albumin excretion (UAE)
(µg/24h)
25
20
15
10
5
0
*
***
ns
*
WT (Vehicle)
WT (STZ)
ST2 -/- (Vehicle)
ST2 -/- (STZ)

Figure 2:

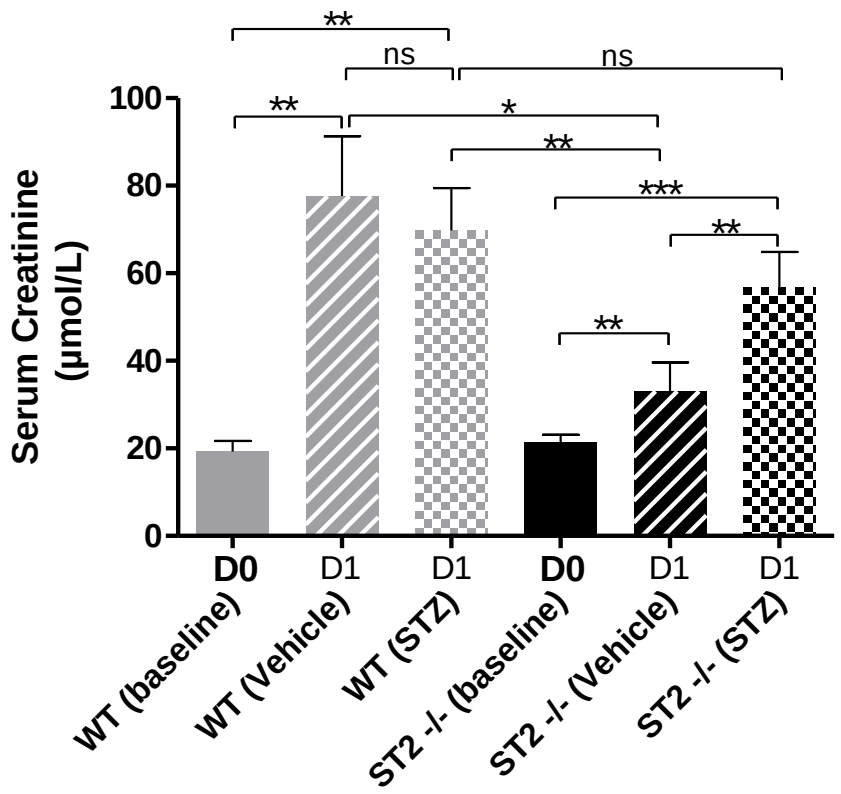
**
ns
ns
**
*
**
***
**
**
100
80
60
40
20
0
Serum Creatinine (µmol/L)
D0
D1
D1
D0
D1
D1
WT (baseline)
WT (Vehicle)
WT (STZ)
ST2 -/- (baseline)
ST2 -/- (Vehicle)
ST2 -/- (STZ)

Figure 3:

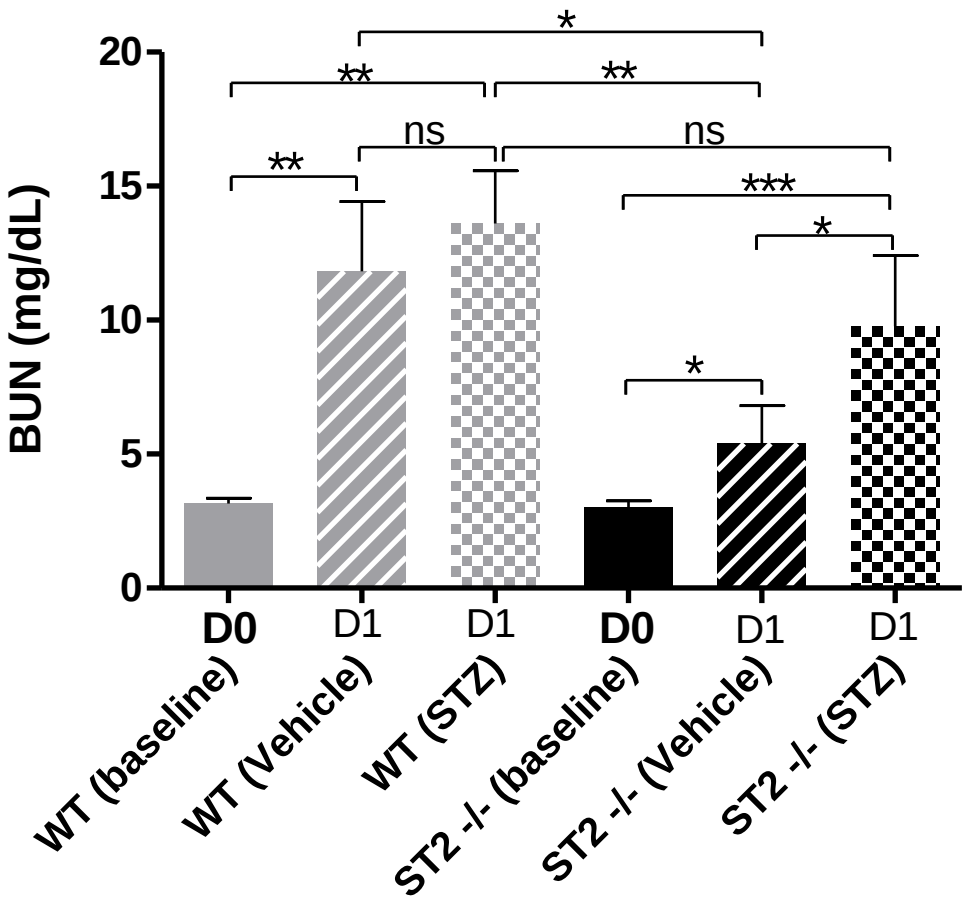
BUN (mg/dL)
20
15
10
5
0
*
**
**
ns
ns
**
***
*
*
D0
D1
D1
D0
D1
D1
WT (baseline)
WT (Vehicle)
WT (STZ)
ST2 -/- (baseline)
ST2 -/- (Vehicle)
ST2 -/- (STZ)

Figure 4:

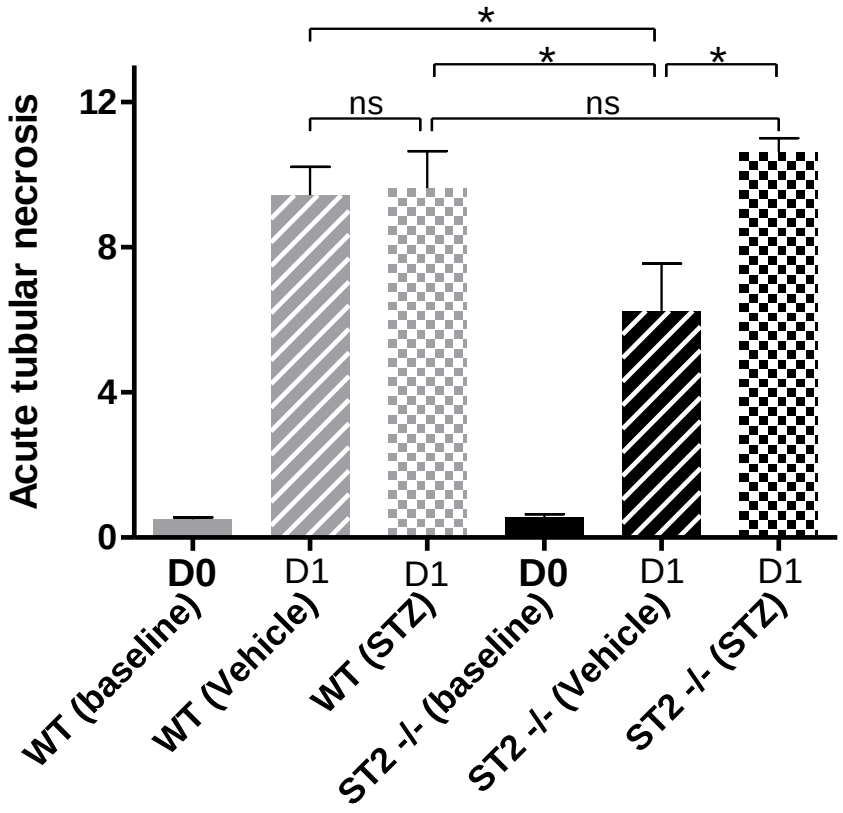
Acute tubular necrosis
12
8
4
0
*
*
*
ns
ns
D0
D1
D1
D0
D1
D1
WT (baseline)
WT (Vehicle)
WT (STZ)
ST2 -/- (baseline)
ST2 -/- (Vehicle)
ST2 -/- (STZ)

Figure 5:

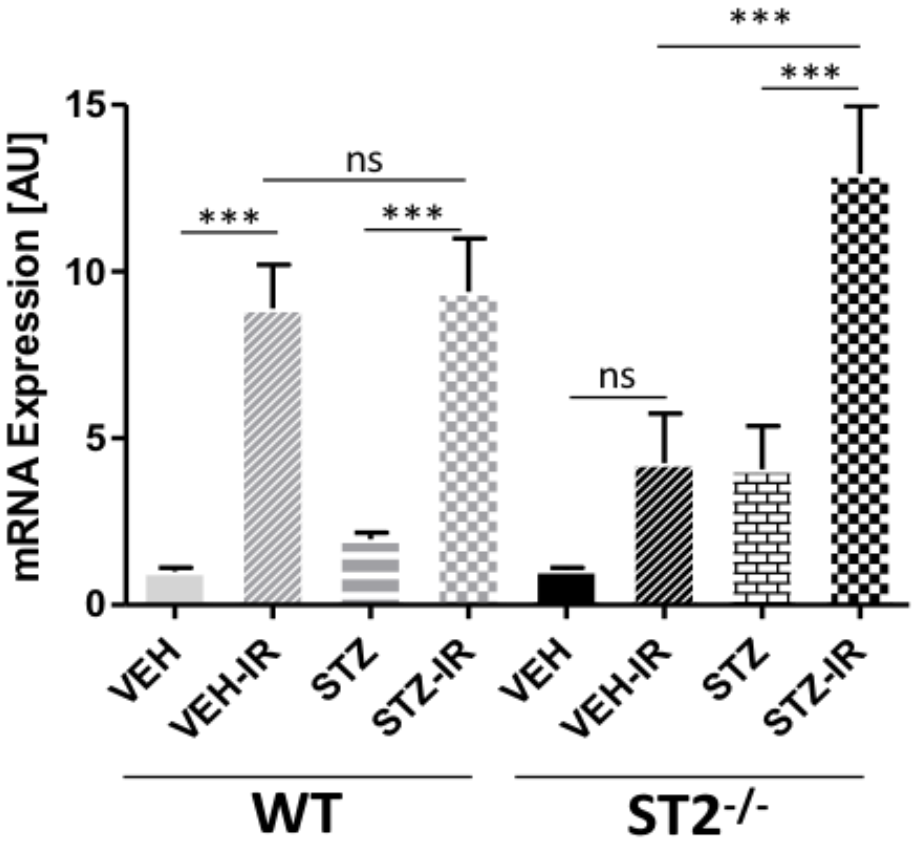
mRNA Expression [AU]
15
10
5
0
***
***
ns
ns
***
***
VEH
VEH-IR
STZ
STZ-IR
VEH
VEH-IR
STZ
STZ-IR
WT
ST2-/-

Gene Name
Gene Sequence of forward and reverse primers (5'→ 3')
Amplicon size (base pair, bp)
GenBank Accession Number

Interleukin 33, Mus musculus (*IL33*)
Forward: CTACTGCATGAGACTCCGTTCTG
Reverse: AGAATCCCGTGGATAGGCAGAG
136 bp
NM_001164724

Monocyte Chimioattractant Protein-1, Mus musculus (*MCP-1/CCL-2*)
Forward: CTGCTGTTCACAGTTGCCG
Reverse: CATTCCTTCTTGGGGTCAGC
218 bp
NM_011333.3

Vascular Endothelial Growth Factor A, Mus musculus (*Vegfa*)
Forward: CTGCTGTAACGATGAAGCCCTG
Reverse: GCTGTAGGAAGCTCATCTCTCC
119 bp
NM_001025250

Primer pairs were designed based on GenBank reference sequences. We used the Primer BLAST interface from NCBI. Unless specified, each primer-pair is separated at least by one intron on the corresponding genomic DNA. To avoid non-specific amplifications, primer sequences were blasted against mouse genes. Dissociation curves were analyzed and agarose gels were run for all primer-pairs to ensure single product amplification.

Supplementary Figure 1

A

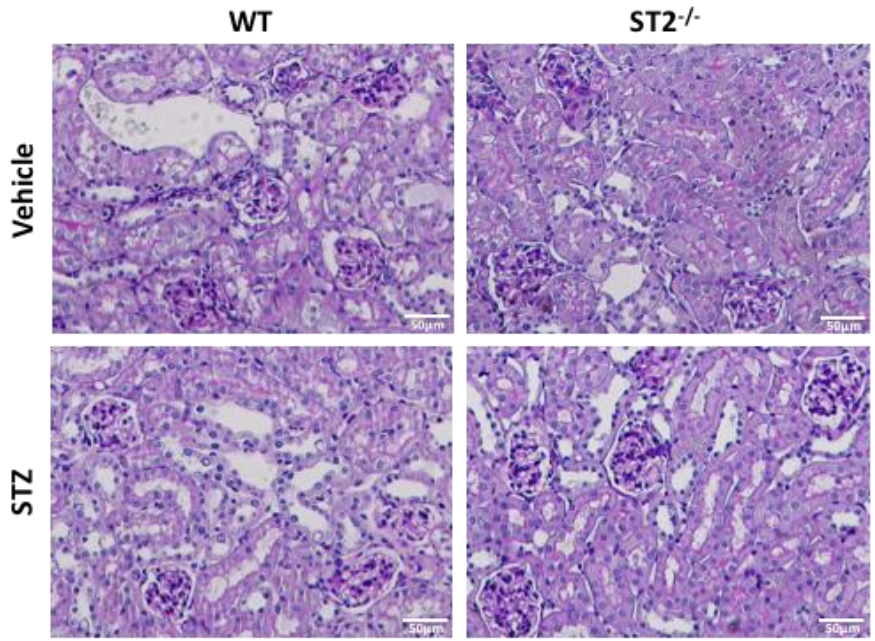

B

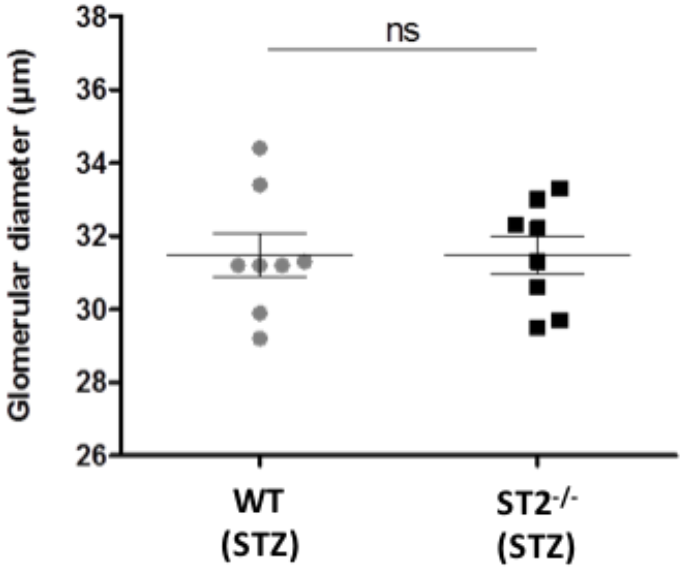

Supplementary Figure 2

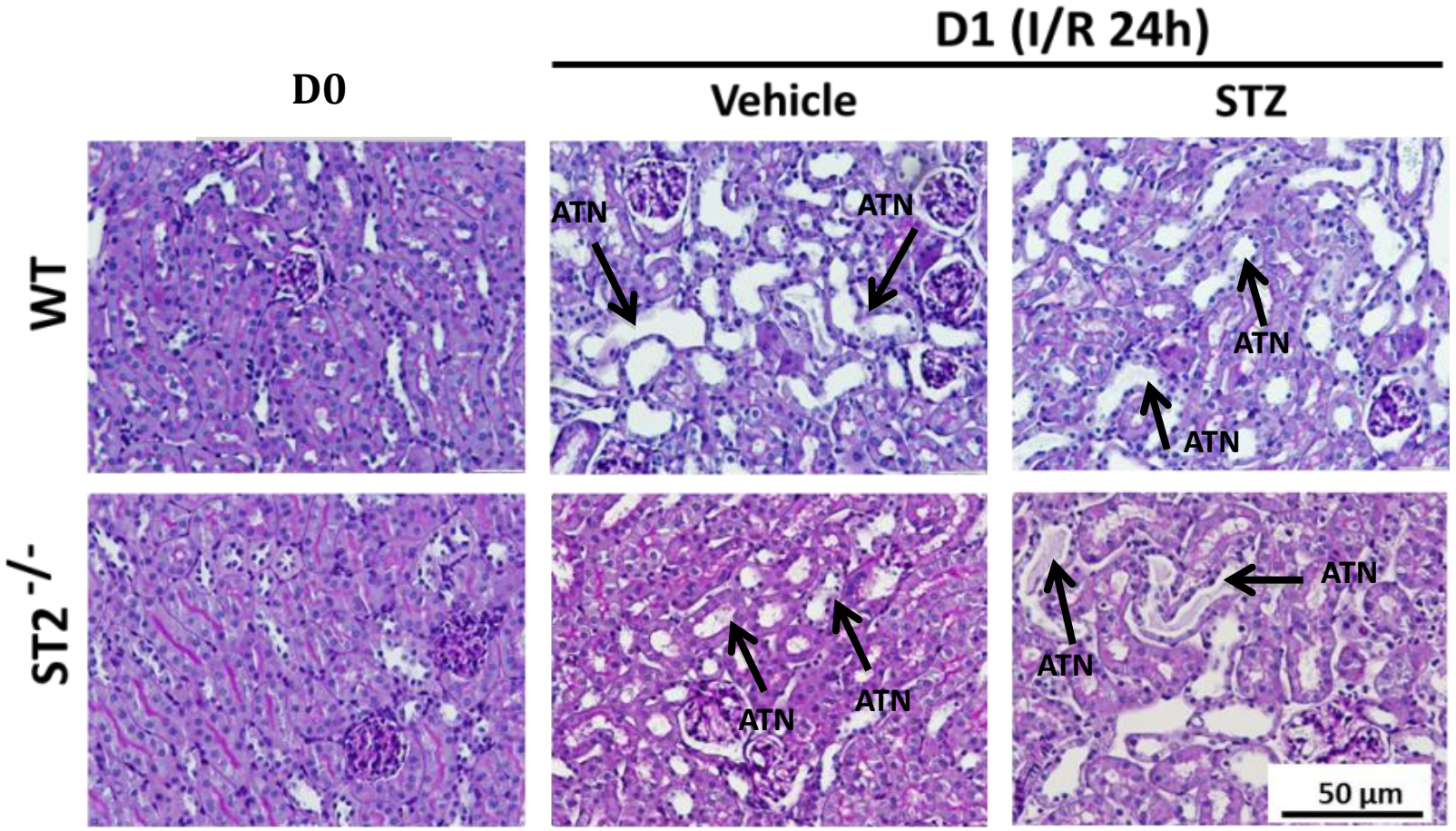

Supplementary Figure 3